



Non-equilibrium atmospheric pressure microplasma jet: An approach to endoscopic therapies

Xiao Zuo, Yu Wei, Long Wei Chen, Yue Dong Meng, and Plasma Medicine Team

Citation: *Physics of Plasmas* (1994-present) **20**, 083507 (2013); doi: 10.1063/1.4817958

View online: <http://dx.doi.org/10.1063/1.4817958>

View Table of Contents: <http://scitation.aip.org/content/aip/journal/pop/20/8?ver=pdfcov>

Published by the [AIP Publishing](#)

Articles you may be interested in

[Chemically reactive species in liquids generated by atmospheric-pressure plasmas and their roles in plasma medicine](#)

AIP Conf. Proc. **1545**, 214 (2013); 10.1063/1.4815857

[DNA damage in oral cancer cells induced by nitrogen atmospheric pressure plasma jets](#)

Appl. Phys. Lett. **102**, 233703 (2013); 10.1063/1.4809830

[Atmospheric-pressure air microplasma jets in aqueous media for the inactivation of *Pseudomonas fluorescens* cells](#)

Phys. Plasmas **20**, 053501 (2013); 10.1063/1.4803190

[Reactive oxygen species-related plasma effects on the apoptosis of human bladder cancer cells in atmospheric pressure pulsed plasma jets](#)

Appl. Phys. Lett. **101**, 053703 (2012); 10.1063/1.4742742

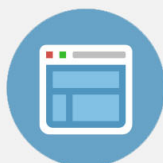
[Highly effective fungal inactivation in He + O₂ atmospheric-pressure nonequilibrium plasmas](#)

Phys. Plasmas **17**, 123502 (2010); 10.1063/1.3526678



Re-register for Table of Content Alerts

Create a profile.



Sign up today!



Non-equilibrium atmospheric pressure microplasma jet: An approach to endoscopic therapies

Xiao Zuo, Yu Wei, Long Wei Chen,^{a)} Yue Dong Meng, and Plasma Medicine Team
 Institute of Plasma Physics, Chinese Academy of Sciences, Hefei 230031, People's Republic of China

(Received 20 April 2013; accepted 22 July 2013; published online 9 August 2013)

Atmospheric pressure microplasma jet generated in a long hollow core optical fiber is studied to verify the potential feasibility of endoscopic therapies. Thermal damage and electric shock to the human body were suppressed by two technical methods, i.e., the high-voltage resistant flexible tube wrapped on the optical fiber and a power resistor of 100 k Ω connected between the power supply and the copper foil electrode. Optical emission spectra analysis indicated that many kinds of active radicals like excited atomic O and OH, were generated in the microplasma jet. In addition, the applications of the microplasma jet on sterilization and lung cancer cell apoptosis were presented. After 5 min of exposures to the microplasma jet, the cell viability and the bacillus subtilis replication decreased to about 3% and zero, respectively. More investigations are needed to improve the plasma-aided endoscopic therapies. © 2013 AIP Publishing LLC. [<http://dx.doi.org/10.1063/1.4817958>]

I. INTRODUCTION

In recent years, non-equilibrium atmospheric pressure plasmas have attracted much attention because they can offer a cheaper and more convenient substitute for low-pressure plasmas.^{1–3} Various configurations and applications of non-equilibrium micro-plasma sources have been extensively investigated. A.A.H. Mohamed *et al.*⁴ developed a DC atmospheric pressure microplasma jet (APMPJ) operated in air, nitrogen and oxygen with the temperature of around 350 K and the length of around 1.5 cm. T. L. Ni *et al.*⁵ designed APMPJ with a pin-hole electrode powered by a 1 kHz voltage source. R. Pothiraja *et al.*⁶ studied a pulsed APMPJ with a voltage of 0–20 kV and a pulse frequency of 4–500 kHz. Y. Shimizu *et al.*⁷ prepared gold nano particles using pulsed APMPJ via inductive coupling at ultra high frequency (UHF, 450 MHz). J. Kim *et al.*⁸ used 2.45 GHz microwave to excite an APMPJ based on the micro-strip technology. APMPJ treatments have been investigated for multiple biological applications,^{9–12} because the small-sized plasma jet could be targeted very specifically to a desired biological site with the lessened risk of contamination, necrosis, inflammation, or scarring in comparison to conventional therapeutic methods. J. Y. Kim *et al.*¹³ used a flexible optical fiber based single-electrode APMPJ to induce apoptosis of lung carcinoma cells, murine melanoma B16F0 tumor cells and fibroblast CL7 cells. Applications as plasma-aided endoscopy for cancer therapies in human body also gathered much attention owing to the excellent characteristics.¹⁴ Micheal Keidar *et al.*¹⁵ reported that the cold plasmas jet could selectively ablate some kinds of cancer cells, while leaving normal cells unaffected. However, problems such as electric shock and thermal damage to the human body need to be overcome.^{16,17} The electric shock and thermal damage are mainly caused by the high voltage (HV) and the rapid increase of the electric current when the microplasma jet

contacts with the biological site to be treated. To solve these problems, we developed a single electrode APMPJ device for plasma endoscopy.

This paper is organized as follows. In Sec. II, we will present some descriptions of the experimental setup and normal working condition of the APMPJ. In Sec. III, experimental results of the application of APMPJ on sterilization and lung cancer cell apoptosis will be shown, and the relevant mechanism is also discussed. Finally, a short summary is given in Sec. IV.

II. EXPERIMENTAL SETUP

The setup of the non-equilibrium APMPJ is schematically shown in Fig. 1. Compared with the conventional dielectric barrier discharge (DBD), hollow cathode discharge and ICP micro-jet, the configuration of the flexible hollow core optical fiber based device is relatively simple. The device consists of three main parts, i.e., the gas supply part (the green dash line block in Fig. 1), the plasma energizing part (the red dash line block in Fig. 1), and the microplasma jet configuration part (the blue dash line block in Fig. 1), respectively. The optical fiber was wrapped with high voltage resistant flexible silica tube so that the tube could be handheld. A flow divider was utilized to guide the gas flowing from a big tube to the micro-size hollow core optical fibers. The inner diameter of the optical fibers was about 300 μm . A piece of 1 cm wide copper foil rotated on the optical fiber served as the high voltage electrode. The length from the HV electrode to the optical orifice was about 30 cm. The microplasma jet was terminated by a virtual ground plane. The HV electrode was connected to the sinusoidal voltage power supply through a 100 k Ω resistor, which could prevent an electrical shock and thermal damage to the human body by decreasing the voltage and electric current upon the desired biological site. High purity (5N) helium was used as the working gas, and a mass flow controller (MFC) was applied to set the gas flow rate below the limit for a laminar flow. When helium flowed through the hollow core optical

^{a)}Electronic mail: lwchen@ipp.ac.cn. Telephone: +86-551-65593308.

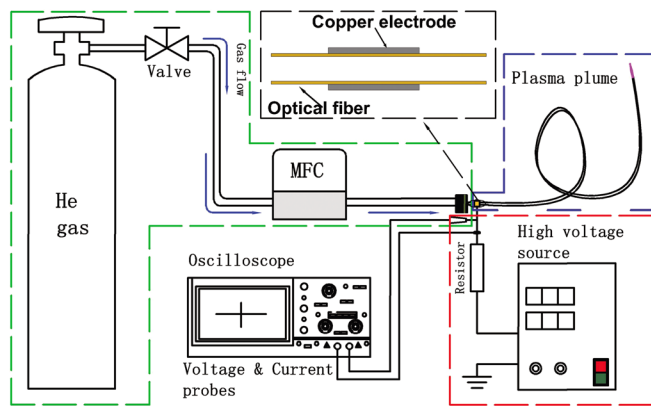


FIG. 1. The schematic of the APMPJ setup.

fiber with a sufficient HV and proper frequency applied, a plasma jet ignited in the fiber was launched into the surrounding air. The experimental parameters are listed in Table I.

The current and high voltage probes were connected directly to the powered electrode to collect current and voltage signals, which were recorded by a digital oscilloscope (Tektronix DPO7104). Analysis of the optical emission spectrum (OES) is an effective method to identify the various reactive species generated by the atmospheric pressure helium microplasma jet. Spectrometer (Acton SP300i) equipped with a charge-coupled device camera with the exposure time of 200 ms was used to analyze the active particles and radicals. A non-contact infrared thermometer (Raynger[®] ST[™]) was adopted to measure the temperature of tissue surfaces when they were exposed to the APMPJ.

III. RESULTS AND DISCUSSION

As shown in Fig. 2, the room temperature APMPJ was handheld and contacted by human finger kindly. The top-left subfigure showed the copper foil electrode on the optical fiber. The helium gas flow rate and the peak voltage applied on the copper electrode was around 1.0 standard-state cubic liter per minute (SLM) and 5.0 kV in the working condition, respectively. The length of the APMPJ in the air was measured about 6 mm. The single electrode microplasma jet could contact with the water in a Petri dish, which meant that it could treat materials without establishing any conductive pathway. Fig. 2 implied that the long and narrow microplasma jet could be directed deeply towards target surfaces with no harm to living organism.

Temporal dynamics of the applied voltage and the discharge current were shown in Fig. 3. When the output peak

TABLE I. The parameters for the helium microplasma jet experiments.

| Parameters (units) | Experimental conditions |
|--|-------------------------|
| Power frequency (kHz) | ~60 |
| Peak output voltage (kV) | 5.0–5.5 |
| Helium flow rate (standard-state cubic liter per minute) | ~1.0 |
| Inner diameter of optical fiber (μm) | ~300 |
| Outer diameter of the probe (mm) | 1.0–2.0 |
| Length of the optical fiber (mm) | ~300 |

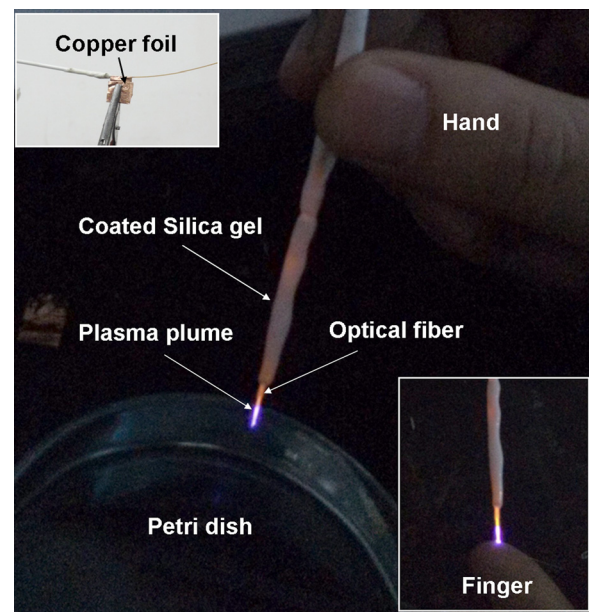


FIG. 2. Photograph of the helium micro-jet plasma held by a hand to contact water in a Petri dish. A silica gel layer was coated outside the optical fiber tube.

voltage was 5.5 kV, the measured discharge current without the resistor in the circuit was about 37.1 mA, while the current with a 100 k Ω resistor in the circuit was only about 15.8 mA. The resistor lowered the discharge current down apparently. After the ignition of plasma in the optical fiber, the peak voltage applied on the copper coil electrode was calculated about 4 kV by subtracting the voltage drop on the resistor. Through this kind of design, the APMPJ could work stably in a lower voltage environment after a high ignition voltage.

In Fig. 4, the applied voltages on electrode and measured currents were compared under two different conditions: the APMPJ contacted with a bare finger and without. The 100 k Ω resistor was utilized in both experiments. It could be found that with a finger contacted with the microplasma jet, the peak voltage on the electrode and the measured peak

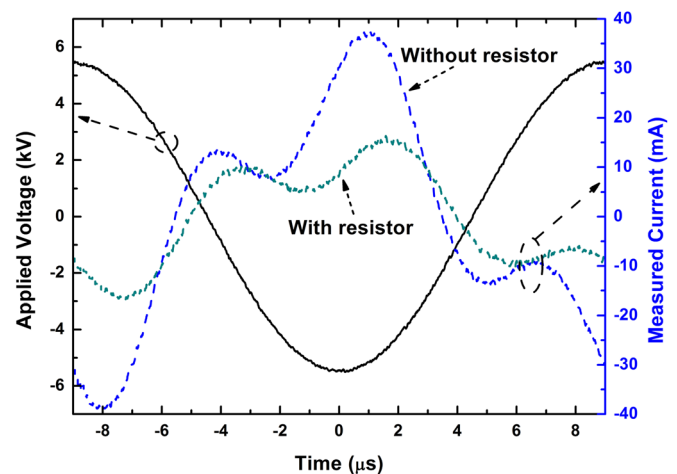


FIG. 3. Temporal dynamics of the applied voltage and the current with/without resistor. The solid line and the dash line represent the applied voltage and the measured current, respectively.

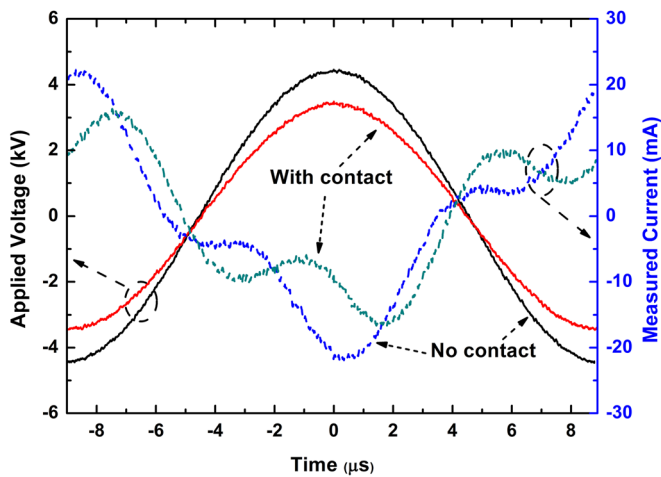


FIG. 4. Temporal dynamics of the voltage and the current with/without finger contact. The solid line and the short dashed line represented the applied voltage and the measured current, respectively.

current both decreased. The HV electrode could induce charges on the local surface of human finger to form a capacitor-like configuration. While voltage between the electrode and the finger was high enough, the capacitor would breakdown and the finger would suffer from electric shock. When the finger contacted with the plasma, the measured current should be increased. However, the voltage on the resistor increased if there was a power resistor, which therefore reduced the voltage on the electrode. As a response, the discharge current decreased lower than that without a resistor. Finally, the power resistor successfully limited the sudden increase in electric current. Therefore, it could be used to prevent the finger from electrode shock and thermal damage.

To certify that the thermal damage to tissues could be avoided by the power resistor, a piece of biological tissue was treated by the APMPJ. Simultaneously, the surface temperature of the tissue was measured by a non-contact infrared thermometer. The peak voltage and the gas flow rate were about 5.5 kV and 1.0 SLM, respectively. The tissue was placed 3 mm away from the optical fiber orifice. Fig. 5 shows

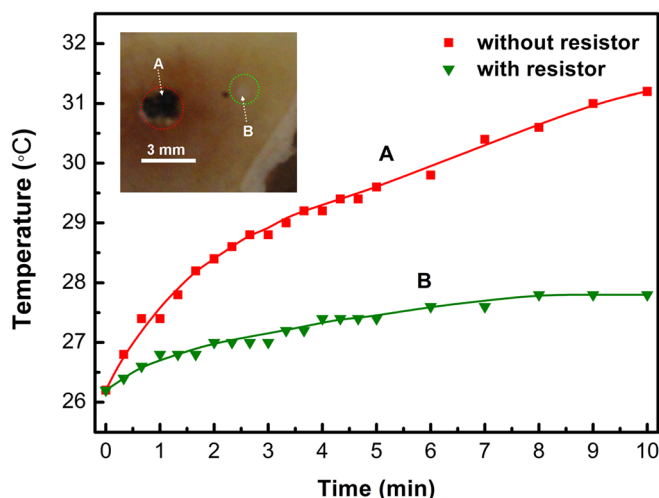


FIG. 5. The temperature increase of the tissue surface exposed to the APMPJ with (line B)/without resistor (line A).

the measured temperature versus the treatment time by the APMPJ with and without a power resistor, respectively. The red line without a resistor was assigned as A and the green line with a resistor was assigned as B. The temperature increased with the treatment time, and reached the steady state with a temperature of 27.6 °C in about 6 min when a 100 kΩ resistor was used. With the initial temperature of 26.2 °C, it increased by 1.4 °C after the APMPJ treatment. However, without the protection of the resistor, the temperature increased much faster and higher. In 3 min the surface of the tissue was destroyed by the thermal heating from the APMPJ. Therefore, the electric shock and thermal damage could be avoided by the introduction of the 100 kΩ resistor between the power source and electrode.

To illustrate the active species contained in the APMPJ and demonstrate the feasibility of the applications of the APMPJ on sterilization, the related OES diagnostics and sterilization experiments were presented. Fig. 6 showed the optical emission spectrum from 200 to 800 nm when 1.0 SLM helium gas was injected. It clearly indicated that excited atomic O, He, meta-stable molecular O₂, N₂ and N₂⁺ exist in the APMPJ with its opening to the ambient air.¹⁸ The emission spectrum was mainly dominated by the presence of excited nitrogen species. In addition to these primary species, hydroxyl (OH) radical with high concentration was detected. These highly reactive species such as OH at 309.01 nm and atomic oxygen at 777.2 nm are considered to be the most effective species in attacking cells or organic material in general, and will play essential roles in medicinal and biomedical applications of non-equilibrium APMPJ.¹⁹

Due to the low energies needed for the rotational excitation and short transition time in diatomic gases discharging, molecules in the rotational states and the neutral gas molecules are in equilibrium. The gas temperature can be estimated by the simulation of the N₂⁺ spectra in the optical spectroscopy. The simulation software Lifbase was used to simulate a N₂⁺ spectrum.²⁰ As shown in the inset graph in Fig. 6, the vibrational temperature and the rotational temperature were estimated about 3000 K and 300 K, respectively. The low temperature characteristics make the APMPJ feasible in most biomedical applications.

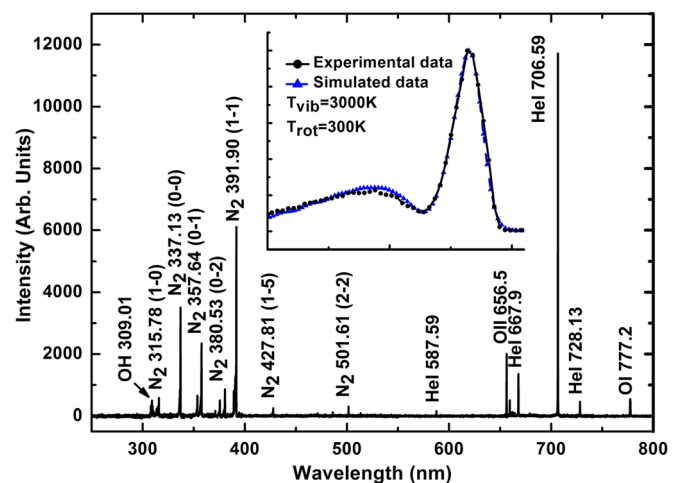


FIG. 6. Optical emission spectra of the APMPJ from 200 nm to 800 nm.

This kind of single electrode APMPJ was also used to inactivate bacteria to investigate its germicidal effects. The direct treatment utilized the tissue itself as an electrode that participated in creating the plasma.²¹ Fridman²² reported that the effect of charged particles on plasma played the essential role in the interaction with living organisms as well as UV radiation. Since our interest was primarily in the sterilization of bacteria to demonstrate the feasibility of the sterilization by the APMPJ with the two protections, the *Bacillus subtilis* was selected as the sample. It is a kind of Gram-positive bacteria, and hard to be inactivated. Fig. 7 showed the photograph of the *Bacillus subtilis* sample treated by the helium APMPJ with the treatment time of 5 min. The size of dark spot expanded larger than the dimension of the optical fiber orifice. Since it was believed that the charged particles could play a significant role in the rupture of the outer membrane of bacterial cells. The electrostatic force caused by charge accumulation could overcome the tensile of the membrane and result in its rupture.⁹ In this experiment, the helium APMPJ was actually in direct contact with the *Bacillus subtilis*. Meanwhile, various activated neutrals, O and OH radicals also played a crucial role in the plasma inactivation process.

In Fig. 8, the variation of cultured lung cancer cell (A549) viability with treatment time by the exposure to the APMPJ was shown. Helium and its mixture with oxygen were used as working gas, respectively. The schematic experimental structure was shown at the bottom-left of the figure. The distance between the Petri dish and the APMPJ is about 1 mm. The viability of the treated A549 cells was analyzed by the cell viability analyzer (Vi-cell). As can be seen from Fig. 8, in the first half minute, the A549 cells viability decreased by 30% after exposure to the mixture gas microplasma jet. However, only 17% reduced by the pure helium microplasma jet. Through 2 min treatment, the mixture gas still showed much better sterilization effect than pure helium gas. Finally, the A549 viability decreased to about 3% after 5 min of exposures to the APMPJ. In comparison with the

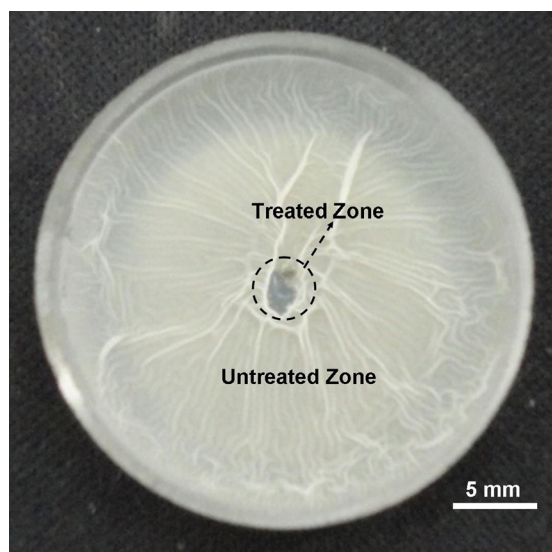


FIG. 7. *Bacillus subtilis* were exposed for 5 min by the micro-jet plasma. The dark zone in the dash circle is the “kill zone”, where bacteria were destroyed and not able to replicate or multiply. The white area is the untreated zone, where bacteria replicated well.

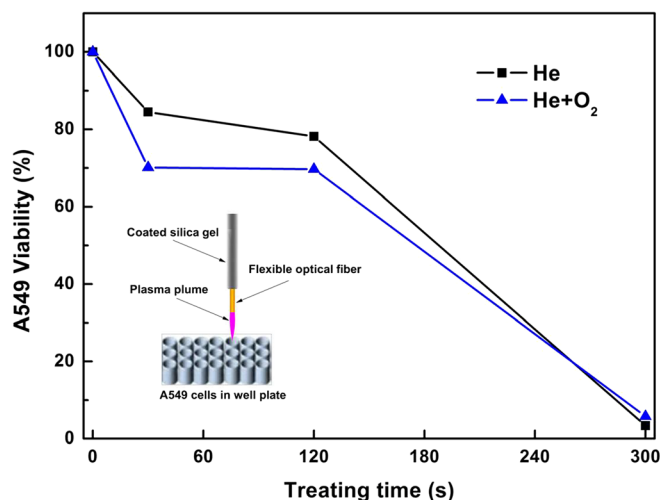


FIG. 8. Variation of A549 viability with treating time by the APMPJ.

helium microplasma jet, the mixture gas microplasma jet represented a better result during lung cancer cells inactivation due to the more concentration of active species like atom O.²³ The experimental results demonstrated the feasibility of the use of APMPJ in killing lung cancer cells.

IV. CONCLUSIONS

In summary, an approach for endoscopic therapies by APMPJ at room temperature was presented. The length from the electrode to the optical fiber orifice and the outer diameter of the probe was around 30 cm and 1.0 mm, respectively, which could make it suitable to treat complex and deep objects like endoscopic application. An HV resistant and flexible silica tube wrapped upon the optical fiber prevented the desired biological site from electric shock when the optical fiber transmitted inside of the human body. By utilizing a power resistor of 100 k Ω connected in series between the power supply and the copper foil electrode, the rapid increase of the electric current was efficiently suppressed when the APMPJ contacted with human organism. Experiment results showed that the added resistor successfully limited the thermal damage and electric shock to the biological tissue. The OES analysis indicated that highly reactive species like atomic O, N₂ excited species, and ozone existed in the plasma plume, which therefore potentially offered an effective and low cost method to treat yeast infections on skin, surface modification, thermally sensitive materials, vulnerable biological materials, and sterilization. In addition, applications of the APMPJ on sterilization and lung cancer cell apoptosis indicated the feasibility of sterilization after the usage of the two methods. These results showed that the hollow core optical fiber microplasma jet could be used to effectively treat a localized biological site without electrical shock and thermal damage.

ACKNOWLEDGMENTS

The authors would like to thank Professor Jianguang Li for his valuable suggestion and Dr. Lingzhi Bao for his kind support on biological diagnostics. This work was financially

supported by the National Natural Science Foundation of China under Grant No. 11205201.

- ¹K. Tachibana, *IEEE Trans. Electr. Electron. Eng.* **1**, 145 (2006).
- ²A. Schutze, J. Y. Jeong, S. E. Babayan, J. Park, G. S. Selwyn, and R. F. Hicks, *IEEE Trans. Plasma Sci.* **26**, 1685 (1998).
- ³L. W. Chen, P. Zhao, X. S. Shu, J. Shen, and Y. D. Meng, *Phys. Plasmas* **17**, 083502 (2010).
- ⁴A. A. H. Mohamed, J. F. Kolb, and K. H. Schoenbach, *Eur. Phys. J. D* **60**, 517 (2010).
- ⁵T. L. Ni, F. Ding, X. D. Zhu, X. H. Wen, and H. Y. Zhou, *Appl. Phys. Lett.* **92**, 241503 (2008).
- ⁶R. Pothiraja, N. Bibinov, and P. Awakowicz, *J. Phys. D: Appl. Phys.* **43**, 495201 (2010).
- ⁷Y. Shimizu, K. Kawaguchi, T. Sasaki, and N. Koshizaki, *Appl. Phys. Lett.* **94**, 191504 (2009).
- ⁸J. Kim and K. Terashima, *Appl. Phys. Lett.* **86**, 191504 (2005).
- ⁹X. H. Zhang, D. P. Liu, H. Z. Wang, L. Y. Liu, S. B. Wang, and S. Z. Yang, *Plasma Chem. Plasma Process.* **32**, 949 (2012).
- ¹⁰B. Gweon, M. Kim, D. B. Kim, D. Kim, H. Kim, H. Jung, J. H. Shin, and W. Choe, *Appl. Phys. Lett.* **99**, 063701 (2011).
- ¹¹H. Ayan, E. D. Yildirim, D. D. Pappas, and W. Sun, *Appl. Phys. Lett.* **99**, 111502 (2011).
- ¹²X. P. Lu, Z. H. Jiang, Q. Xiong, Z. Y. Tang, and Y. Pan, *Appl. Phys. Lett.* **92**, 151504 (2008).
- ¹³J. Y. Kim, J. Ballato, P. Foy, T. Hawkins, and S. O. Kim, *IEEE Trans. Plasma Sci.* **39**, 2958 (2011).
- ¹⁴J. Y. Kim, J. Ballato, P. Foy, T. Hawkins, Y. Z. Wei, J. H. Li, and S. O. Kim, *Biosens. Bioelectron.* **28**, 333 (2011).
- ¹⁵M. Keidar, A. Shashurin, O. Volotskova, M. A. Stepp, P. Srinivasan, A. Sandler, and B. Trink, *Phys. Plasmas* **20**, 057101 (2013).
- ¹⁶G. Cho, J. Kim, H. Kang, Y. Kim, G. C. Kwon, and H. S. Uhm, *J. Appl. Phys.* **112**, 103305 (2012).
- ¹⁷G. Cho, H. Kang, E. Choi, and H. S. Uhm, *IEEE Trans. Plasma Sci.* **41**, 498 (2013).
- ¹⁸R. W. B. Pearse and A. G. Gaydon, *The Identification of Molecular Spectra*, 4th ed. (Chapman and Hall, London, 1976).
- ¹⁹M. Laroussi and T. Akan, *Plasma Processes Polym.* **4**, 777 (2007).
- ²⁰J. Luque and D. R. Corsley, SRI International Report No. MP 99-009, (1999).
- ²¹J. Y. Kim, J. Ballato, P. Foy, T. Hawkins, Y. Z. Wei, J. H. Li, and S. O. Kim, *IEEE Trans. Plasma Sci.* **39**, 2974 (2011).
- ²²G. Fridman, A. D. Brooks, M. Balasubramanian, A. Fridman, A. Gutsol, V. N. Vasilets, H. Ayan, and G. Friedman, *Plasma Processes Polym.* **4**, 370 (2007).
- ²³S. J. Kim, T. H. Chung, S. H. Bae, and S. H. Leem, *Appl. Phys. Lett.* **94**, 141502 (2009).